

The X-ray Cluster Dipole

M. Plionis¹ & V. Kolokotronis²

¹ National Observatory of Athens, Lofos Nimfon, Thessio, 18110 Athens, Greece

² Astronomy Unit, School of Mathematical Sciences, Queen Mary and Westfield College, Mile End Road, London E1 4NS

ABSTRACT

We estimate the dipole of the whole sky X-ray flux-limited sample of Abell/ACO clusters (XBACs) and compare it to the optical cluster dipole which is known to be well aligned with the CMB dipole and which converge to its final value at $\sim 160h^{-1}$ Mpc (Branchini & Plionis 1996 and references therein). The X-ray cluster dipole is well aligned ($\lesssim 25^\circ$) with the CMB dipole, while it follows closely the radial profile of its optical cluster counterpart although its amplitude is $\sim 10 - 30$ per cent lower. In view of the fact that the the XBACs sample is not affected by the volume incompleteness and the projection effects that are known to exist at some level in the optical parent Abell/ACO cluster catalogue, our present results confirm the previous optical cluster dipole analysis that there are significant contributions to the Local Group motion from large distances ($\sim 160h^{-1}$ Mpc). In order to assess the expected contribution to the X-ray cluster dipole from a purely X-ray selected sample we compare the dipoles of the XBACs and the Brightest Cluster Sample (Ebeling et al. 1997a) in their overlap region. The resulting dipoles are in mutual good agreement with an indication that the XBACs sample slightly underestimates the full X-ray dipole (by $\lesssim 5$ per cent) while the Virgo cluster contributes about 10 - 15 per cent to the overall X-ray cluster dipole. Using linear perturbation theory to relate the X-ray cluster dipole to the Local group peculiar velocity we estimate $\beta_{cx} (\equiv \Omega_o^{0.6}/b_{cx}) \simeq 0.24 \pm 0.05$.

Subject headings: X-ray clusters: clustering – large scale structure of Universe – gravitational acceleration field

1. Introduction

A lively debate has been going on the recent years on which is the spatial extent of the distribution of mass inhomogeneities that cause the LG motion. Assuming gravitationally instability as the cause of cosmic motions and using as tracers of the matter distribution optical

and IR galaxies, many studies (cf. Yahil, Walker & Rowan-Robinson 1986; Harmon et al. 1987; Lahav 1987; Lahav, Rowan-Robinson & Lynden-Bell 1988; Lynden-Bell, Lahav & Burstein 1989; Strauss et al. 1992; Hudson 1993) have shown that most, if not all, of the peculiar acceleration of the LG is induced within $40 - 50h^{-1}$ Mpc. Other analysis of galaxy samples have presented indications, of varying strength, for contributions from much larger depths, ranging from $\sim 100h^{-1}$ Mpc to $\sim 150h^{-1}$ Mpc (Plionis 1988; Rowan-Robinson et al. 1990; Plionis, Coles & Catelan 1993; Vasilakos & Plionis 1997). However the difficulty with such studies in providing a definite answer is that the galaxy samples are not volume limited but rather magnitude- or flux-limited which introduces an inherent uncertainty due to the rapid decrease of their selection function with distance from the observer.

Alternatively, galaxy clusters being the largest gravitationally-collapsed structures in the universe and luminous enough to be volume-limited out to large distances have also been used to probe the local acceleration field. Existing studies, all based on the optically selected Abell/ACO clusters (Abell, Corwin & Olowin 1989) provide strong evidence that the LG dipole has significant contributions from depths up to $\sim 160h^{-1}$ Mpc (Scaramella, Vettolani & Zamorani 1991; Plionis & Valdarnini 1991; Branchini & Plionis 1996). However, due to the the volume incompleteness of richness class $R=0$ clusters (cf. Peacock & West 1992) and to optical projection effects (enhancement of galaxy density along the direction of foreground rich clusters which cause inherently poor background clusters or groups to appear rich enough to be included in the sample), these results should be verified by well defined cluster samples, free of such biases.

In the X-ray band the physical reality of clusters is unquestionable due to their strong ICM X-ray emission. Two large X-ray cluster samples have been recently compiled; the XBACs sample by Ebeling et al. (1996), from carefully cross-correlating the ROSAT all-sky X-ray survey (Trümper 1990; Voges 1992) with the Abell/ACO cluster sample and the Brightest Cluster Sample (BCS) by Ebeling et al. (1997a) from an additional cross-correlation of the RASS sources with the Zwicky cluster catalogue but it also contains clusters purely selected in X-rays (for the complete definition see section 2.2). The XBACs sample provides, for the first time, a whole sky, flux-limited, sample of X-ray galaxy clusters suitable for investigating the local acceleration field (for an early attempt using mostly HEAO-1 data see Lahav et al. 1989). The BCS sample covers only the northern sky and it has been used to investigate the evolution of the X-ray cluster luminosity function (Ebeling et al. 1997b) while both samples will be useful for establishing, among other things, the cluster correlation function (Edge et al. in preparation). Nevertheless, both catalogues suffer from some degree of incompleteness at low galactic latitude (see also sections 2.3 and 3 for relative corrections). Apart from these two samples, other X-ray cluster samples, also based on ROSAT data, are under compilation, most notably the ESO KP catalogue for southern clusters (Collins et al. 1995; de Grandi 1996; Guzzo et al. 1995, 1996).

As in the case of all flux-limited samples, the use of these X-ray cluster samples to investigate the very distant contributions to the local acceleration field is limited exactly due to their flux-limited nature. In fact Kolokotronis et al. (1997) found, using numerical experiments, that such samples will underestimated the true underlying cluster dipole by ~ 15 per cent on average if such distant contributions do exist. We further caution the reader that using clusters to estimate the local acceleration field maybe problematic because:

- Clusters may not trace well the very local gravity field due to their large intercluster separation ($\sim 30 - 40h^{-1}$ Mpc) and unless the local velocity field is cold, which does seem to be the case (cf. Peebles 1988), attempts to relate the cluster dipole with the LG peculiar velocity could give erroneous results.
- Existing cluster samples are incomplete in many different ways. For example the Virgo cluster is missing from the optical Abell/ACO catalogue and thus also from the XBACs sample. Furthermore, the present X-ray cluster samples may suffer from incompleteness in the nearby Universe due to problems in reliably detecting extended low-surface brightness emission.

These limitations will be investigated by comparing, in their overlap region, the XBACs and BCS dipoles, since the latter sample is nearer to being purely X-ray selected and it also contains the Virgo cluster.

The outline of this paper is as follows. The X-ray samples and various selection biases are discussed in section 2. The main dipole results are presented in section 3, while in section 4 we estimate the cosmological β parameter. Finally, our main conclusions are presented in section 5.

2. X-ray samples & selection effects

Both X-ray samples consist of clusters identified in the ROSAT all sky survey (RASS) by a combination of two detection algorithms (the Standard Analysis Software System and Voronoi Tessellation Percolation; SASS and VTP hereafter) for fluxes above a particular flux limit (S_{lim}). The use of the VTP identification algorithm allows quite reliable cluster detections even at low redshifts and improves greatly the flux determination for the X-ray sources, initially misassessed by SASS (see Ebeling et al. 1996; 1997a and references therein for superiority of VTP over SASS technique).

Throughout this work we will be using the following definition of distance (Mattig’s formula):

$$r = \frac{c}{H_0 q_0^2 (1+z)} \left[q_0 z + (1 - q_0)(1 - \sqrt{2q_0 z + 1}) \right]$$

with $q_0 = 0.5$ and $H_0 = 100h \text{ km s}^{-1} \text{ Mpc}^{-1}$.

2.1. XBACs sample

The XBACs sample consists of the X-ray brightest Abell/ACO clusters that have been detected in the ROSAT all sky survey (RASS) for fluxes above $S_{\text{lim}} = 5 \times 10^{-12} \text{ erg s}^{-1} \text{ cm}^{-2}$ (0.1 - 2.4 keV) with redshifts limited by $z \leq 0.2$. The sample contains 253 clusters out of which 242 have $|b| \geq 20^\circ$ and thus it is the largest X-ray flux-limited cluster sample to date (though not entirely X-ray selected). The X-ray fluxes measured initially by the SASS point source detection algorithm are superseded by VTP measurements that account for the extended nature of the emission. In addition, the difficulty of the SASS algorithm to actually detect nearby X-ray emission has been mostly corrected by running VTP on the RASS fields centered on the optical positions of all nearby Abell/ACO clusters ($z \leq 0.05$) irrespective of whether or not they are detected by SASS. Ebeling et al. (1996) estimate, after a careful analysis of possible selection effects and biases that the overall completion rate of this X-ray sample is more than 80 per cent.

2.1.1. XBACs systematic effects

Due to the cross-correlation of the RASS with the Abell/ACO cluster positions, it is very probable that the systematic biases from which the latter suffer, could also creep in the XBACs sample. Ebeling et al. (1996) have shown that the XBACs flux-limited sample is free of the known volume incompleteness, as a function of distance, of the richness class $R=0$ Abell/ACO clusters, exactly because of the flux-limited property of the XBACs sample which is such, that it contains at large distances the inherently brighter and thus richer Abell/ACO clusters for which there is no volume incompleteness.

Another bias from which the optical clusters suffers and which could therefore affect also the XBACs sample, is the significant distance dependent density variations between the northern Abell and southern ACO parts of the combined cluster sample (cf. Batuski et al. 1989; Scaramella et al. 1990; Plionis & Valdarnini 1991). These density variations are most probably due to the higher sensitivity of the ACO IIIa-J emulsion plates which results in detections of inherently poorer nearby ACO clusters. As a first step to quantify the overall magnitude of the effect on the XBACs sample we estimate, for $|b| > 30^\circ$, the density ratio and its Poisson error between the Abell and ACO parts of the sample within the volume limited region of the optical cluster sample;

$$\frac{\bar{n}_{\text{ACO}}}{\bar{n}_{\text{Abell}}}(r < 240h^{-1} \text{ Mpc}) \simeq \begin{cases} 1.56 \pm 0.14 & \text{optical} \\ 1.12 \pm 0.17 & \text{XBACs} \end{cases}$$

where each cluster has been weighted by $\mathcal{P}(b)(\equiv 10^{\mathcal{A} \cos \epsilon |b|})$, to account for the number density decrease due to Galactic absorption¹. It is evident that the X-ray selection has corrected the significant systematic density variation seen in the optical sample. The lower X-ray detection rate of ACO clusters is probably because they are inherently poorer clusters (and thus weak X-ray emitters), revealed due to the higher sensitivity of the IIIa-J emulsion ACO plates.

As already mentioned, the apparent density variations between the Abell and ACO samples are distance dependent (Plionis & Valdarnini 1991) and since uncorrected systematic density differences between two parts of the sky can introduce spurious contributions to the dipole, we will statistically correct such variations by weighting each Abell cluster with:

$$w(r, \delta V_i) = \frac{\bar{n}_{\text{ACO}}(r, \delta V_i)}{\bar{n}_{\text{Abell}}(r, \delta V_i)} \quad (1)$$

The robustness of our results will be checked by using a large number of bin sizes (δV_i). Note that due to small number statistics the density variations may be non-significant and thus we will be using $w(r) = 1$ whenever $\sigma(w) \geq |1 - w(r)|$.

2.2. BCS sample

The BCS is the biggest X-ray selected, X-ray flux-limited compilation covering the extragalactic sky in the northern hemisphere ($\delta \geq 0^\circ$, $|b| \geq 20^\circ$). It contains 199 clusters above $S_{\text{lim}} = 4.45 \times 10^{-12} \text{ erg s}^{-1} \text{ cm}^{-2}$, in the same energy band as the XBACs, with $z \leq 0.3$ and with X-ray luminosities $\geq 1.25 \times 10^{42} h^{-2} \text{ erg s}^{-1}$. The BCS list includes not only Abell clusters but also the brightest Zwicky clusters and others selected on the basis of their X-ray properties alone. It therefore has a significant overlap with XBACs (for $\delta \geq 0^\circ$) as far as the Abell population is concerned. The above BCS sample is estimated to be 90 per cent complete (redshift completion is more than 96 per cent).

2.3. X-ray cluster selection functions

Necessary in estimating the local acceleration field from flux-limited samples is the use of the sample selection function which is determined in our case by the cluster X-ray luminosity function, $\Phi_x(L)$. Ebeling et al. (1997c; 1997b) have recently fitted to the data a Schechter luminosity

¹The amplitude of this function has been estimated from each individual cluster sample and it is consistent with the usually quoted values ($\mathcal{A}_{\text{Abell}} \simeq -0.3$ and $\mathcal{A}_{\text{ACO}} \simeq -0.2$).

function (with parameters given in Table 1):

$$\Phi_x(L) = A \exp\left(-\frac{L}{L_*}\right) L^{-\alpha}, \quad (2)$$

where L_* is the characteristic luminosity measured in $10^{44} h^{-2} \text{ erg s}^{-1}$, A being the overall normalization of the number-density measured in $h^3 \text{ Mpc}^{-3} (10^{44} h^{-2} \text{ erg s}^{-1})^{\alpha-1}$, and α is the usual power-law index.

The selection function, defined as the fraction of the cluster number density that is observed above the flux limit at some distance r , is:

$$\phi(r) = \frac{1}{\bar{n}_c} \int_{L_{\min}(r)}^{L_{\max}} \Phi_x(L) dL. \quad (3)$$

with $L_{\min}(r) = 4\pi r^2 S_{\text{lim}}$ and $L_{\max} \simeq 10^{45} h^{-2} \text{ erg s}^{-1}$ (due to the form of $\Phi_x(L)$ the above integral is very insensitive to larger values of L_{\max}). The mean number density of the underlying X-ray population of clusters is found by integrating the luminosity function from the lower to the upper luminosity limit of the sample:

$$\bar{n}_c = \int_{L_{\min}}^{L_{\max}} \Phi_x(L) dL. \quad (4)$$

Since L_{\min} , the absolute lower luminosity limit, for the XBACs sample is effectively unknown we can estimate it by relating the above equation with the observed number density of the optical Abell/ACO sample which can be considered as the ‘parent’ population of the XBACs sample. Using the weighted mean number density of Abell/ACO clusters, corrected for Galactic absorption ($\bar{n}_c \simeq 1.85 \text{ }^{+0.6}_{-0.3} \times 10^{-5} h^3 \text{ Mpc}^{-3}$) we obtain $L_{\min} = 4.3 \text{ }^{+3.5}_{-2.5} \times 10^{41} h^{-2} \text{ erg s}^{-1}$; the uncertainty reflecting the density variations between the Abell and ACO samples. For the case of the BCS sample, for which $L_{\min} = 1.25 \times 10^{42} h^{-2} \text{ erg s}^{-1}$, we obtain that the global mean number density of its parent X-ray cluster population is $\bar{n}_c = 5.81 \times 10^{-5} h^3 \text{ Mpc}^{-3}$, a factor of ~ 3 times larger than that of the XBACs sample.

The predicted number of X-ray clusters above S_{lim} and lying within a shell between r and $r + \Delta r$, is then:

$$N(r) = 4\pi r^2 \phi(r) \bar{n}_c \Delta r = 4\pi r^2 \Delta r \int_{L_{\min}(r)}^{L_{\max}} \Phi_x(L) dL \quad (5)$$

Note that $N(r)$ is independent of \bar{n}_c and thus of the uncertainty in L_{\min} . Fig. 1 shows the observed number of XBACs clusters as a function of distance and the predicted one from equation (5). The maximum of $N(r)$ turns out to be around $\sim 240 h^{-1} \text{ Mpc}$, in agreement with the observed distribution. If we choose to fit better only the region of reliable redshifts ($\lesssim 0.1$) we would obtain for the luminosity function parameters: $\alpha \approx 1.25$ and $L_* \approx 1.2 \times 10^{44} h^{-2} \text{ erg s}^{-1}$ (dashed line in fig. 1), which although deviate from the nominal values of Table 1, they are within their 1σ uncertainty. The insert of fig. 1 shows the corresponding $N(r)$ of the optical Abell/ACO cluster,

corrected for Galactic absorption (stars) and the theoretical curve for the range of Abell and ACO densities.

Fig. 2 presents the observed BCS $N(r)$ distribution, for $|b| \geq 30^\circ$, and the corresponding theoretical one (equation 5). The maximum of the selection function turns out to be at $\sim 140h^{-1}$ Mpc, followed by a long tail towards larger depths. This early maximum ensures that the BCS function is dominated by relatively local clusters, more so than the corresponding XBACs sample.

Note that we will limit our dipole analysis within $240h^{-1}$ Mpc to avoid possible systematic effects due to the low number of the observed X-ray clusters and due to uncertainties in the $m_{10} - z$ based cluster redshifts that dominate above this depth.

3. Cluster Dipole

We will not present all the details of the method used to calculate the peculiar gravitational acceleration induced by some mass tracer on the observer since such can be found in many recent articles (cf. Tini-Brunozzi et al. 1995; Kolokotronis et al. 1996 and references therein). Briefly, we employ the method of moments to quantify the distribution of clusters around the LG and we correct them for the effects of galactic absorption using a spherical harmonic expansion of the cluster surface number density and a combined mask to take into account the depletion of clusters for $|b| < 13^\circ$ and a cosec b absorption law above this latitude limit (see Plionis & Valdarnini 1991 and the appendix of Tini-Brunozzi et al. 1995 for details). We then estimate the gravitational acceleration induced on the LG from the distribution of X-ray clusters (cf. Miyaji & Boldt 1990; Plionis et al. 1993) by:

$$\mathbf{V}_g(r) = H_o r \frac{\mathbf{D}}{\mathcal{M}}(\leq r) \quad \text{for } r \geq R_{\text{conv}} \quad (6)$$

where $\mathbf{D} = \sum \mathcal{W}_i r_i^{-2} \hat{\mathbf{r}}_i$ is the dipole, $\mathcal{M} = \sum \mathcal{W}_i r_i^{-2}$ is the monopole, $\mathcal{W}_i (\propto w_i \phi_i^{-1} M_i)$ are the cluster weights with M_i an estimate of the cluster mass, ϕ_i the cluster selection function and w_i the Abell/ACO relative weight (see equation 1). R_{conv} is the dipole convergence depth, the depth beyond which the distant density inhomogeneities do not affect the dynamics of the observer and should therefore be within the effective depth of the catalogue in order to obtain the correct estimate of the local acceleration field. Using the definition of the monopole ($\mathcal{M} = \int \rho(r) r^{-2} dV$) and linear perturbation theory (cf. Peebles 1980) we can recover from equation (6) the more familiar form:

$$\mathbf{u}_{\text{LG}}(r) = \beta_{\text{cx}} \mathbf{D}(r) / 4\pi \bar{n}_c = \beta_{\text{cx}} \mathbf{V}_g(r) . \quad (7)$$

where $\beta_{\text{cx}} \equiv \Omega_o^{0.6} / b_{\text{cx}}$ and b_{cx} is the X-ray cluster to underlying mass bias factor. Note that we will be using two mass weighting schemes; one in which we will assume each cluster to contribute

equally ($M = 1$) and one in which the mass is proportional to the X-ray luminosity ($M \propto L_x^{5/11}$). This relation results from the assumption of hydrostatic equilibrium, $T \propto M^{2/3}$, and from GINGA observations which indicate that $L_x \propto T^{3.3}$ (cf. Arnaud 1994 and references therein).

The sparseness, however, with which the flux-limited sample of clusters trace their underlying parent cluster population introduces shot-noise (discreteness effects) in their dipole estimates which increase with distance. Kolokotronis et al. (1997) found that the enhancement of the underlying true cluster X-ray dipole due to shot-noise and the loss of dipole signal due to the flux-limited nature of the sample work in opposite directions, tending to counteract each other. Therefore, although we estimate the magnitude of the 1D shot-noise dipole, using the formalism developed in Strauss et al. (1992), i.e. $|\mathbf{D}|_{\text{sn,1D}}^2 \approx 1/3 \sum \phi_i^{-1} r_i^{-4} (\phi_i^{-1} - 1)$, finding it to be about ~ 30 per cent of the dipole signal, we do not attempt to correct the *raw* XBACs dipole for such effects (see also Hudson 1993 and Kolokotronis et al. 1997 for alternative shot-noise definitions).

3.1. Dipole Results

In fig. 3 we present the cluster dipole (based on both mass weighting schemes) for the XBACs sample (triangles) as well as for the optical Abell/ACO sample (squares). It is evident that both samples exhibit a very similar dipole profile with significant contributions from depths $\gg 100h^{-1}$ Mpc, which validates the previous results based only on the optical sample (Plionis & Valdarnini 1991; Scaramella, Vettolanni & Zamorani 1991; Branchini & Plionis 1996). However, the XBACs dipole is systematically lower, by ~ 20 per cent (for the equal mass weighting case), than the optical cluster dipole. Although this could be intrinsic, implying that the optical dipole is artificially enhanced by projection effects (cf. Sutherland 1988; Peacock & West 1992), such an explanation is not corroborated by the correlation function analysis of the XBACs sample which provides a large correlation length, roughly consistent with that of the optical Abell/ACO sample (Edge, private communication). An alternative explanation of the lower XBACs dipole amplitude with respect to the optical one, is a possibly artificial exclusion from the XBACs catalogue of nearby clusters ($\lesssim 50 - 60h^{-1}$ Mpc) which naturally play a key role in shaping the local acceleration field. In fact, from the 8 Abell/ACO clusters within $60h^{-1}$ Mpc not included in the XBACs sample, three (A3565, A3574 and A347), although detected in RASS, have been excluded because of suspicion that their X-ray emission is mostly of non-cluster origin. If we include by hand these three clusters, then the XBACs ($M = 1$) dipole increases substantially, reducing the difference with the optical dipole from ~ 20 to ~ 10 per cent. This reduced discrepancy could be further gapped if we take into account the results of Kolokotronis et al. (1997) who found, using numerical experiments, that the cluster X-ray flux-limited and unity weighted ($M = 1$) dipole will underestimate by ~ 15 per cent the underline cluster dipole if it has significant contributions

from large depths ($\gg 100h^{-1}$ Mpc).

However, using the more natural luminosity weighting scheme ($M \propto L_x^{5/11}$) we find an even lower amplitude of the XBACs dipole with respect to the unity weighted one, although their dipole profiles are very similar. The amplitude of the luminosity weighted X-ray cluster dipole is by ~ 35 per cent less than its optical counterpart and although the ~ 25 per cent gap could be bridged, as discussed above, it seems that the X-ray cluster dipole is intrinsically less, by $\gtrsim 10$ per cent, than the optical cluster dipole. This difference, if it is indeed intrinsic, corresponds to an optical to X-ray cluster bias factor $b_{o,x}(\equiv b_o/b_x) > 1$.

In order to further investigate these points we will attempt to fill in the lack of local information by using the BCS clusters, which better trace the local volume (see fig. 2) and compare the XBACs and BCS dipoles in their common region ($\delta > 0^\circ$, $|b| > 20^\circ$). One's hope is that at the convergence depth of the XBACs dipole the relative fluctuation between the BCS and XBACs dipoles will reflect those of the whole-sky dipole, and therefore we could infer a better estimate of the final X-ray cluster dipole amplitude.

3.2. Comparing the XBACs and BCS dipoles

The northern XBACs sample (hereafter XBACs-n) contains 113 clusters out of which 112 belong to the BCS sample as well, with A2637 being the sole exception (for details see section 10 of Ebeling et al. 1997a). Furthermore, although 65 per cent of the clusters of the two samples are common, it is not straight-forward that they should trace similarly the northern hemisphere dipole since (a) the BCS is governed by a significantly different $\Phi_x(L)$ which results in a different $N(r)$ distribution (see figs. 1 and 2) and (b) only ~ 33 and ~ 53 per cent of the clusters are common within the interesting regions (~ 100 and $\sim 200 h^{-1}$ Mpc respectively).

For this comparative work we will correct the raw dipole estimates for shot-noise errors since the two samples should trace the same underlying distribution but with different densities and selection functions. We plot in the lower panel of fig. 4 the fluctuations of the unity weighted XBACs-n and BCS dipoles ($\delta V/V \equiv V_{\text{XBACs-n}} - V_{\text{BCS}}/V_{\text{BCS}}$) including (dashed line) and excluding Virgo (solid line). We also plot (upper panel) the misalignment angle between the XBACs-n and BCS dipoles at each distance bin for the luminosity weighted one (solid line) and for the unity-weighted dipole case (long dashed line) excluding Virgo. The short dashed line corresponds to the luminosity weighted dipoles but including in the BCS sample the Virgo cluster.

The most significant results of this analysis are:

- Comparing consistently the BCS and XBACs-n dipoles, i.e. excluding Virgo from the BCS

sample since by construction it is absent from the XBACs, we find that both X-ray samples have very similar dipole shapes, with small amplitude differences ($\delta V/V \lesssim 0.05$) and $\delta\theta \lesssim 14^\circ$ at scales $\gtrsim R_{\text{conv}}$. Note that the $\delta\theta$ values are uncorrected for the misalignment induced by the shot noise dipole, which is roughly $\sim 10^\circ$.

- If one takes into account the above value of the relative velocity difference between the BCS and the XBACs-n one would further reduce the apparent gap between the XBACs all-sky and the optical Abell/ACO dipole but by not more than ~ 5 per cent.
- Similarly with the XBACs also in the BCS case the luminosity weighted dipole is by ~ 20 per cent lower than the corresponding unity weighted one.
- Including Virgo in the BCS sample we find, as expected, that it plays a significant role in shaping the X-ray dipole, with relative contribution of $\sim 10 - 15$ per cent which corresponds to an average Virgocentric infall velocity of $\sim 160 \pm 40$ km/sec (were we have weighted twice the luminosity based results).

4. Estimating the density parameter β

The good alignment (within $\sim 25^\circ$) between the XBACs and CMB dipoles indicate that the XBACs clusters trace the large-scale mass density field and that they can therefore be used to estimate the cosmological β parameter by relating the X-ray cluster dipole to the Local Group peculiar velocity (equation 7). However since the Virgo cluster is not included in the Abell sample, due to its proximity and thus low surface density, we must exclude from the LG peculiar motion the Virgocentric Infall. Equation (7) then becomes:

$$\mathbf{u}'_{\text{LG}} = \mathbf{u}_{\text{LG}} - \mathbf{V}_{\text{inf}} = \beta_{\text{cx}} |\mathbf{V}_{\text{g}}|. \quad (8)$$

Using $V_{\text{inf}} \simeq 170 \text{ km s}^{-1}$ we find $|\mathbf{u}'_{\text{LG}}| \simeq 500 \text{ km s}^{-1}$, pointing towards $(l, b) = (265^\circ, 15^\circ)$.

The cluster redshift is related to its the comoving distance by:

$$cz = H_0 r + [\mathbf{v}_p(r) - \mathbf{u}_{\text{LG}}] \cdot \hat{\mathbf{r}} \quad (9)$$

and since the last term of this equation is $\neq 0$, redshift-space distortions will tend to enhance the dipole amplitude (Kaiser 1987). In an attempt to derive the optical cluster dipole free of such distortions, Branchini & Plionis (1996) used a density reconstruction algorithm to predict the real-space positions of the optical Abell/ACO clusters. They found that redshift space distortions (*r.s.d* hereafter) enhance the real-space optical cluster dipole by ~ 23 per cent. In order to correct the XBACs dipole for such effects we attempt to minimize *r.s.d* using a simple model of

the peculiar velocity field. Since we observe in the local Universe a coherent bulk flow of high amplitude (cf. Dekel 1994, 1997; Strauss & Willick 1995), we split the cluster peculiar velocities in a component of a bulk flow and a local non-linear component as follows:

$$\mathbf{v}_p(r) = \mathbf{V}_{\text{bulk}}(r) + \mathbf{V}_{\text{nl}}(r) \quad (10)$$

Applying equation (10) to the Local Group and using equation (8) we have that $\mathbf{V}_{\text{bulk}}(0) = \mathbf{u}'_{\text{LG}}$ from which it is evident that locally the bulk flow component dominates over that of the infall. This fact may be reversed for galaxies at large distances but in any case at such distances we have $(\mathbf{v}_p \cdot \hat{\mathbf{r}})/cz \ll 1$ and thus *r.s.d* should not significantly affect the dipole. We therefore use the approximation $\mathbf{v}_p(r) = \mathbf{V}_{\text{bulk}}(r)$, where the bulk flow profile, as a function of distance, is given by Dekel (1994, 1997) and by Branchini, Plionis & Sciamia (1996), and its direction is taken to be that of $\mathbf{V}_{\text{bulk}}(0)$. Note, however, that there have been measurements of the bulk velocity with very different results from the above in direction as well as in amplitude (Lauer & Postman 1994). The reality, however, of these results have been questioned by different studies (cf. Giovanelli et al 1996; Hudson & Ebeling 1996).

Our results are completely compatible with those of the full reconstruction of Branchini & Plionis (1996); the redshift-space XBACs dipole is enhanced by ~ 20 per cent with respect to the corrected (*real-space*) dipole. The main dipole results and the corresponding values of β_{cx} (using equation 7) are presented in Table 2. Taking into account a possible ~ 20 per cent artificial decrease of the X-ray dipole (see discussion in 3.1) and averaging over the different determinations (weighting twice the more physical luminosity weighted results) we obtain

$$\beta_{\text{cx}} \simeq 0.24 \pm 0.05 .$$

Note that from the optical Abell/ACO cluster dipole Branchini & Plionis (1996) found $\beta_{\text{co}} \approx 0.21$. Furthermore, Branchini et al. (1997) comparing the real-space optical cluster density field (within $\sim 70h^{-1}$ Mpc) with the corresponding POTENT-Mark III field found $\beta_{\text{co}} \approx 0.20 \pm 0.06$. The difference between their β_{c} value and the present analysis could be attributed to an optical to X-ray cluster bias factor $b_{\text{o,x}} \simeq 1.2$.

5. Conclusions

We have estimated the X-ray cluster dipole, using the whole-sky XBACs sample and the BCS sample which covers the northern hemisphere. We have found that:

- (a) The relative contributions to the LG acceleration field, from different depths, is readily provided by the XBACs dipole analysis and supports the conclusions drawn from the optical

Abell/ACO cluster analysis of significant dipole contributions ($\sim 30 - 40$ per cent of total) from scales $\sim 130 - 160h^{-1}$ Mpc. Furthermore, the XBACs and BCS clusters trace equally well the same dipole structure and thus the large-scale density field.

- (b) Using a model of the large-scale peculiar velocity field and correcting for redshift space distortions, we find that the *real-space* X-ray cluster dipole is reduced by ~ 20 per cent, a value consistent with the outcome of a full reconstruction of the optical cluster density field.
- (c) Although the ‘zero-point’ of the X-ray cluster dipole cannot be unambiguously determined from the present analysis we find that the true underlying X-ray cluster dipole is intrinsically lower than the corresponding optical cluster dipole by ~ 10 to 30 per cent, depending on whether the X-ray clusters are weighted equally or $\propto L_x^{5/11}$ and on whether one assumes that the observed X-ray emission of a few nearby clusters (A3565, A3574 and A347) is of non-cluster origin.
- (d) Relating the X-ray cluster dipole with the LG peculiar velocity we find $\Omega_c^{0.6}/b_{cx} \simeq 0.24 \pm 0.05$, which combined with recent determinations based on comparing the optical cluster density and velocity fields with the corresponding POTENT-Mark III fields, imply a relative optical to X-ray cluster bias factor of $b_{o,x} \simeq 1.2$.
- (e) The Virgo cluster contributes about $\sim 10 - 15$ per cent of the overall X-ray cluster dipole which corresponds to an average Virgocentric infall velocity of $\sim 160 \pm 40$ km/sec.

We greatly thank Harald Ebeling for many useful discussions, for kindly giving us the XBACs & BCS luminosity functions and the BCS sample prior to publication and for always answering meticulously our many questions. We also acknowledge fruitful discussions with Alastair Edge on the statistical properties of the XBACs and BCS samples.

REFERENCES

- Abell G.O., Corwin, H.G., Olowin, R.P., 1989, ApJS, 70, 1
- Arnaud, M., 1994, in W. Seitter ed., Cosmological Aspects of X-ray Clusters of Galaxies, NATO ASI Series, Vol.441, 197
- Batuski D.J., Bahcall N.A., Olowin R.P., Burns J.O., 1989, ApJ, 341, 599
- Branchini E., Plionis M., 1996, ApJ, 460, 569

- Branchini E., Plionis M., Sciama D.W., 1996, *ApJ*, 461, L17
- Branchini E., Plionis M., Zehavi I., Dekel A., 1997, in preparation
- Collins C.A. et al., 1995, in Maddox S.J., Aragon-Salamanca A., eds, *Wide field spectroscopy and the distant universe: The 35th Herstmonceux Conference*. World Scientific, Cambridge, United Kingdom, p. 213
- de Grandi S., 1996, in Zimmermann H.U., Trümper J., eds, *Röntgerstrahlung from the universe: International conference on X-ray Astronomy and Astrophysics*. Würzburg, Germany, p. 577
- Dekel A., 1994, *ARA&A*, 32, 371
- Dekel A., 1997, in L.da Costa ed. ‘Galaxy Scaling Relations: Origins, Evolution & Applications’, Springer, in press
- Ebeling H. et al., 1995, in Maddox S.J., Aragon-Salamanca A., eds, *Wide field spectroscopy and the distant universe: The 35th Herstmonceux Conference*. World Scientific, Cambridge, United Kingdom, p. 221
- Ebeling H., Voges W., Böhringer H., Edge A.C., Huchra J.P., Briel U.G., 1996, *MNRAS*, 281, 799
- Ebeling H., Edge A.C., Fabian A.C., Allen S.W., Crawford C.S., 1997b, *ApJ*, 479, L101
- Ebeling H., Edge A.C., Böhringer H., Allen S.W., Crawford C.S., Fabian A.C., Voges W., Huchra J.P., 1997a, *MNRAS*, submitted
- Ebeling H. et al., 1997c, in preparation
- Edge A. et al., 1997, in preparation
- Giovanelli R., Haynes M.,P., Wegner G., Da Costa L., Freudling W., Salzer J.J., 1996, *ApJ*, 464, L99
- Guzzo L. et al., 1995, in Maddox S.J., Aragon-Salamanca A., eds, *Wide field spectroscopy and the distant universe: The 35th Herstmonceux Conference*. World Scientific, Cambridge, United Kingdom, p. 205
- Guzzo L., 1996, in Coles P., Martinez V.J., Pons-Borderia Maria-Jesus., eds, *Mapping, measuring and modeling the universe*. Astronomical society of the pacific, San Fransisco, California, p. 157
- Harmon R.T., Lahav O., Meurs E.J.A., 1987, *MNRAS*, 228, 5p
- Hudson M.J., 1993, *MNRAS*, 265, 72
- Hudson M.J. & Ebeling H., 1996, *ApJ*, 479, 621
- Kaiser N., 1987, *MNRAS*, 227, 1

- Kolokotronis V., Plionis M., Coles P., Borgani S., Moscardini L., 1996, MNRAS, 280, 186
- Kolokotronis V., Plionis M., Coles P., Borgani S., 1997, MNRAS, submitted
- Lahav O., 1987, MNRAS, 225, 213
- Lahav O., Edge A.C., Fabian A.C., Putney A., 1989, MNRAS, 238, 881
- Lahav O., Rowan-Robinson M., Lynden-Bell D., 1988, MNRAS, 234, 677
- Lauer, T.R. & Postman, M., 1994, ApJ, 425, 418
- Lynden-Bell, D., Lahav, O. & Burstein, D., 1989, MNRAS, 241, 325
- Miyaji T., Boldt E., 1990, ApJ, 353, L3
- Peacock J.A., West M.J., 1992, MNRAS, 259, 494
- Peebles, P.J.E., 1988, ApJ, 332, 17
- Peebles P.J.E., 1980. The Large Scale Structure of the Universe, Princeton University Press, Princeton New Jersey
- Plionis M., 1988, MNRAS, 234, 401
- Plionis M., Valdarnini R., 1991, MNRAS, 249, 46
- Plionis M., Coles P., Catelan P., 1993, MNRAS, 262, 465
- Romer A.K., Collins C.A., Böhringer H., Cruddace R.G., Ebeling H., MacGillivray H.T., Voges W., 1994, Nature, 372, 75
- Rowan-Robinson M. et al., 1990, MNRAS, 247, 1
- Scaramella R., Zamorani, G., Vettolani, G., Chincarini, G., 1990, AJ, 101, 342
- Scaramella R., Vettolani G., Zamorani G., 1991, ApJ, 376, L1
- Sutherland W., 1988, MNRAS, 234, 159
- Strauss M., Yahil A., Davis M., Huchra J.P., Fisher K., 1992 ApJ, 397, 395
- Strauss M.A., Willick J., 1995, Phys. Rep., 261, 271
- Tini Brunozzi P., Borgani S., Plionis M., Moscardini L., Coles P., 1995, MNRAS, 277, 1210
- Trümper J., 1990, Phys. Bl., 46 (5), 137
- Vasilakos S., Plionis M., 1997, in preparation
- Voges W., 1992, Proseedings of Satellite Symposium 3, ESA ISY-3, p. 9
- Yahil A., Walker, D. & Rowan-Robinson, M., 1986, ApJ, 301, L1
- Yahil A., Strauss M., Davis M., Huchra J.P., 1991, ApJ, 372, 380

Tables

Table 1: Parameters for the XBACs and BCS X-ray luminosity function, using $H_0 = 100 h$ km s⁻¹ Mpc⁻¹.

Parameters	XBACs	BCS
A	1.955×10^{-6}	1.246×10^{-6}
α	$1.21^{+0.12}_{-0.13}$	1.85 ± 0.09
L_*	$1.048^{+0.17}_{-0.14}$	$2.275^{+0.515}_{-0.373}$

Table 2: XBACs Dipole Parameters and the corresponding values of β_{cx} at $r = 200 h^{-1}$ Mpc. Note that $\delta\theta_{\text{cmb}}$ is the dipole misalignment angle from the CMB dipole direction corrected for a 170 km s⁻¹ Virgocentric infall.

frame	M	$ \mathbf{V}_g $ (km/sec)	l°	b°	$\delta\theta_{\text{cmb}}$	β_{cx}
z -space	1	2710	269	0	17°	0.19
z -space	$L_x^{5/11}$	2100	275	15	19°	0.24
$real$ -space	1	2250	255	-7	25°	0.22
$real$ -space	$L_x^{5/11}$	1750	251	10	15°	0.29

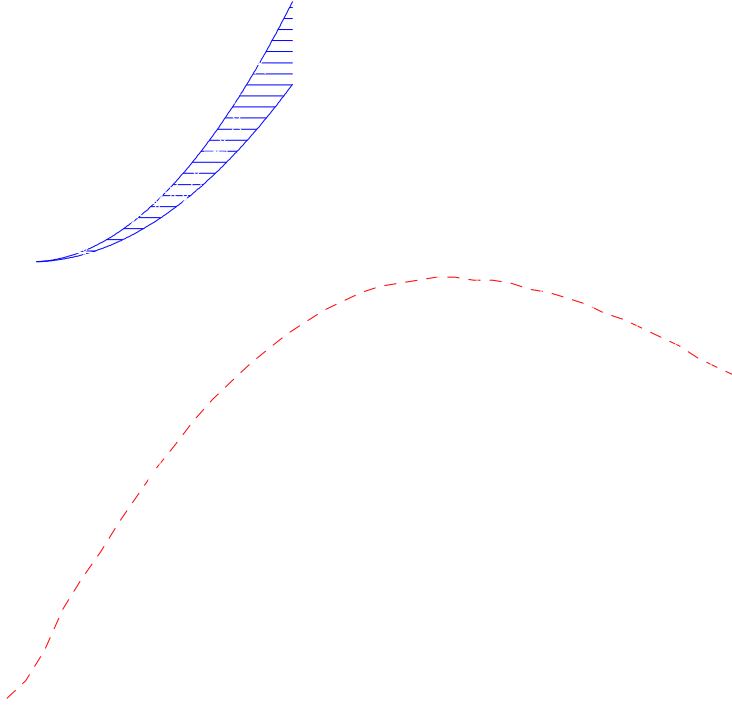


Fig. 1.— Observed $N(r)$ distribution of XBACs clusters, corrected for Galactic absorption, and its Poisson uncertainties. The predicted distribution via equation (5) is shown as a solid line. The insert shows the observed $N(r)$ distribution of the optical Abell/ACO clusters (stars), with the shaded area corresponding to the homogeneous case (i.e. $\phi = 1$) for densities, \bar{n}_c , between the Abell and ACO values.

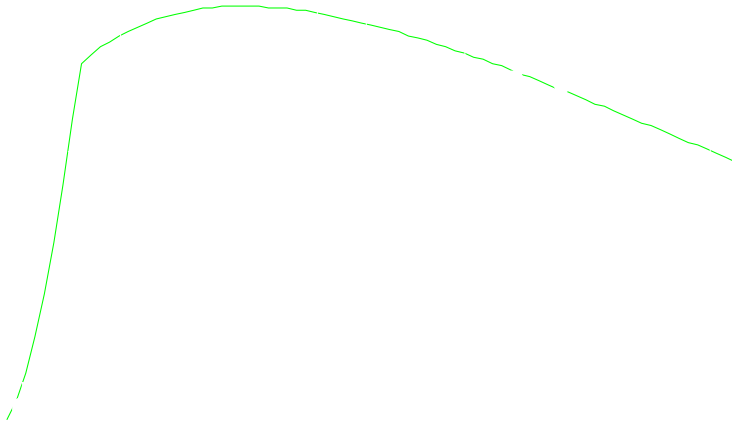


Fig. 2.— Observed $N(r)$ distribution of BCS clusters, corrected for Galactic absorption, and its Poisson uncertainties (points). The predicted distribution via equation (5) is shown as a solid line.

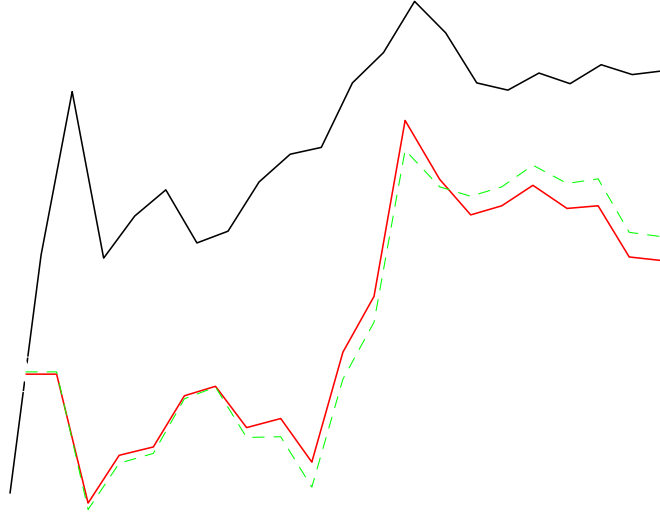


Fig. 3.— Abell/ACO optical (squares) and XBACs (triangles) dipole. The weighting scheme used is indicated. Errorbars are 1σ uncertainties due to different bin sizes used to homogenize the Abell and ACO number densities (see equation 2), while the dashed line is the case with no relative weighting between the Abell and ACO portions of XBACs.



Fig. 4.— Dipole amplitude variation ($\delta V/V$) between BCS and XBAC-n for the unity weighting scheme excluding (solid line) and including Virgo (dashed line). Misalignment angles, $\delta\theta$, where the solid and short-dashed lines correspond to the L_x weighted case excluding and including Virgo, respectively. The long dashed line corresponds to the unity weighted case, excluding Virgo.